Turkish Journal of Science & Technology
18(1), 139-155, 2023

Research Paper
https://doi.org/10.55525/tjst.1212513

An NCA-based Hybrid CNN Model for Classification of Alzheimer's Disease on Grad-CAM-enhanced Brain MRI Images

Feyza ALTUNBEY ÖZBAY[1*], Erdal ÖZBAY[2]
[1] Software Engineering Department, Faculty of Engineering, Firat University, 23119, Elazig, Turkiye
[2] Computer Engineering Department, Faculty of Engineering, Firat University, 23119, Elazig, Turkiye
[*1] faltunbey@firat.edu.tr, [2] erdalozbay@firat.edu.tr

(Geliş/Received: 30/11/2022; Kabul/Accepted: 06/01/2023)

Abstract: Alzheimer's, one of the most prevalent varieties of dementia, is a fatal neurological disease for which there is presently no known cure. Early diagnosis of such diseases and classification with computer-aided systems are of great importance in determining the most appropriate treatment. Imaging the soft tissue of the brain with Magnetic Resonance Imaging (MRI) and revealing specific findings is the most effective method of Alzheimer's diagnosis. A few recent studies using Deep Learning (DL) to diagnose Alzheimer's Disease (AD) with brain MRI scans have shown promising results. However, the fundamental issue with DL architectures like CNN is the amount of training data that is required. In this study, a hybrid CNN method based on Neighborhood Component Analysis (NCA) is proposed, which aims to classify AD over brain MRI with Machine Learning (ML) algorithms. According to the classification results, DenseNet201, EfficientNet-B0, and AlexNet pre-trained CNN architectures, which are 3 architectures that give the best results as feature extractors, were used as hybrids among 10 different DL architectures. By means of these CNN architectures, the features trained on the dataset and the features obtained by Gradient-weighted Class Activation Mapping (Grad-CAM) are concatenated. The NCA method has been used to optimize all concatenated features. After the stage, the optimized features have been classified with KNN, Ensemble, and SVM algorithms. The proposed hybrid model achieved 99.83% accuracy, 99.88% sensitivity, 99.92% specificity, 99.83% precision, 99.85% F1-measure, and 99.78% Matthews Correlation Coefficient (MCC) results using the Ensemble classifier for the 4-class classification of AD.

Key words: Classification, Alzheimer's disease, Grad-CAM, MRI, NCA.

Grad-CAM ile İyileştirilmiş Beyin MRI Görüntülerinde Alzheimer Hastalığının Sınıflandırılması için NCA tabanlı Hibrit CNN Modeli

Öz: Demansın en yaygın türlerinden biri olan Alzheimer, şu anda bilinen bir tedavisi olmayan ölümcül bir nörolojik hastalıktır. Bu tür hastalıkların erken teşhisi ve bilgisayar destekli sistemlerle sınıflandırılması en uygun tedavinin belirlenmesinde büyük önem taşımaktadır. Manyetik Rezonans Görüntüleme (MRI) ile beynin yumuşak dokusunun görüntülenmesi ve spesifik bulguların ortaya çıkarılması Alzheimer teşhisinde en etkili yöntemdir. Beyin MRI taramaları ile Alzheimer Hastalığını (AD) teşhis etmek için Derin Öğrenmeyi (DL) kullanan birkaç yeni çalışma umut verici sonuçlar vermiştir. Ancak, CNN gibi DL mimarileriyle ilgili temel sorun, gereken eğitim verisi miktarıdır. Bu çalışmada, Makine Öğrenimi (ML) algoritmaları ile beyin MRI üzerinden AD'yi sınıflandırmayı amaçlayan Komşuluk Bileşen Analizi (NCA) tabanlı hibrit bir CNN yöntemi önerilmiştir. Sınıflandırma sonuçlarına göre, özellik çıkarıcı olarak en iyi sonuçları veren 3 mimari olan DenseNet201, EfficientNet-B0 ve AlexNet ön-eğitimli CNN mimarileri, 10 farklı DL mimarisi arasından hibrit olarak kullanılmıştır. Bu CNN mimarileri sayesinde, veri seti üzerinde eğitilen öznitelikler ile Gradient-weighted Class Activation Mapping (Grad-CAM) ile elde edilen öznitelikler birleştirilmiştir. NCA yöntemi, tüm birleştirilmiş özellikleri optimize etmek için kullanılmıştır. Bu aşamadan sonra optimize edilen öznitelikler KNN, Ensemble ve SVM algoritmaları ile sınıflandırılmıştır. Önerilen hibrit model, AD'nin 4-sınıflı sınıflandırması için Ensemble sınıflandırıcısını kullanarak %99,83 doğruluk, %99,88 duyarlılık, %99,92 özgüllük, %99,83 kesinlik, %99,85 F1-ölçütü ve %99,78 Matthews Korelasyon Katsayısı (MCC) sonuçlarına ulaşmıştır.

Anahtar kelimeler: Sınıflandırma, Alzheimer hastalığı, Grad-CAM, MRI, NCA.

1. Introduction

Dementia, which is frequently encountered especially in the elderly population, is a general name given to many diseases in which forgetfulness is at the forefront and may occur due to different diseases. Alzheimer's disease (AD) consists of an average of 70% of dementia cases [1]. There is presently no cure for the neurodegenerative disease Alzheimer's, one of the most prevalent types of dementia, which results in the loss of brain cells and a decline in mental abilities [2]. As people age, signs of this disease, which impairs cognition,

* Corresponding author: faltunbey@firat.edu.tr. ORCID Number of authors: [1] 0000-0003-0629-6888, [2] 0000-0002-9004-4802

memory, and behavioral abilities, become more pronounced [3]. Due to the fact that it is a progressive disease, early symptoms of Alzheimer's are usually seen as forgetting recent events, but within a few years, individuals may have difficulty performing their daily activities alone [4].

By 2050, it is anticipated that there would be almost twice as many cases of different types of dementia [5]. Since there is no definitive treatment that stops or slows the progression of the disease, it is vital to provide a solid diagnosis with accurate methods [6]. A brain biopsy is required for definitive diagnosis, but this method is not preferred because it is an invasive procedure [7]. In this regard, Magnetic Resonance Imaging (MRI) is widely used to analyze clinical and neuroimaging findings since it offers more insightful data on cerebral cortical atrophy, even though Computed Tomography (CT) may be favored for illness diagnosis. Since MRI reveals the involvement caused by the loss of volume in some parts of the brain of sick people, it can diagnose the disease at a rate of 90%. However, the inability to detect this volume loss at the onset of AD may lead to underdiagnosis and overlook of the disease [8].

Brain imaging findings are used to analyze the degree of AD in clinically evaluated patients while focusing on features such as medial temporoparietal and temporal lobe atrophy [9]. The volume of the hippocampus, entorhinal cortex (inferior surface of the parahippocampal gyrus), cingulate gyrus, and parietal lobe decreases with medial temporal lobe atrophy, but the parahippocampal fissure enlarges [10]. Early symptoms include parietal atrophy and enlargement of the parietooccipital and posterior cingulate sulcus. As a result, the precuneus' volume increases [11].

Some medical tests are performed for the diagnosis of AD, which results in a large amount of variable heterogeneous data. Due to the nature of these tests, manually analyzing data can be tiring. It is possible for radiologists to make mistakes when interpreting radiological images. In this case, misdiagnosis and treatment of patients become inevitable [12]. Machine Learning (ML) and Deep Learning (DL) applications minimize the occurrence of such errors in medical imaging and especially Computer-Aided Diagnosis (CAD) and allow doctors to increase their experience by easing the workload [13].

Today, deep CNN approaches attract the attention of researchers in the field of computer vision due to their performance in applications such as recognition, detection, classification, and segmentation. In these applications, besides determining the presence or absence of a disease, classification of diseases can also be performed [14]. Feature extraction and visualization in DL applications are important steps that determine the effectiveness of the CAD method. Different features are revealed by texture analysis in images. However, these features alone may be insufficient to determine the accuracy of the model. CNN models are capable of extracting features in a hierarchical fashion, from low to high [15].

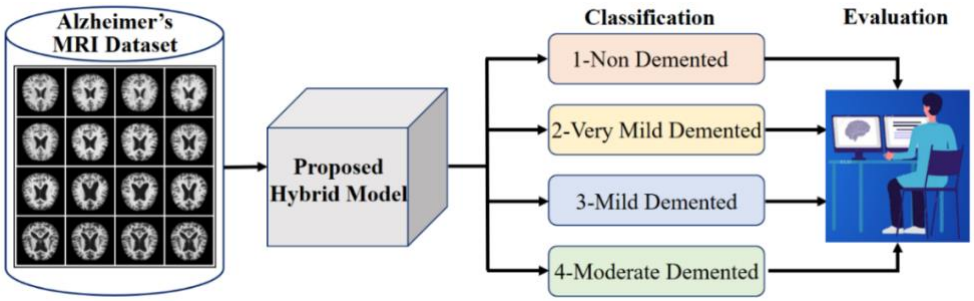

Figure 1. The workflow of the proposed hybrid model

This study aimed to classify the diagnosis of AD according to the stage of dementia, which is a challenging task for specialists since the pixel intensities of the brain MRI images of individuals can be similar. In this respect, brain MRI images were classified with a hybrid model based on DL. Firstly, the features extracted with 10 different CNN architectures were classified with 3 different classifiers. The results obtained here were evaluated comparatively and a hybrid model was created by combining the features obtained from the 3 architectures that gave the highest results using these 10 architectures, and the features obtained using Gradient-weighted Class Activation Mapping (Grad-CAM), a method that reveals distinctive texture features. Then, the best features were selected among the features with the Neighborhood Component Analysis (NCA) method, and these features were classified by KNN, Ensemble, and SVM classifiers. While 98.3% accuracy was achieved with the DenseNet201 + Ensemble model, 97.9% accuracy was achieved with the EfficientNet-B0 + Ensemble model, and 97.1% accuracy was achieved with the AlexNet + Ensemble model, and 99.83% accuracy was achieved with the proposed hybrid model + Ensemble. The workflow of the proposed hybrid model is shown in Fig 1. Unintentional manual

errors can be prevented by reducing the workload of doctors with the proposed method in the diagnosis of AD. Moreover, this method eliminates the need for specialists for preliminary diagnosis.

The significant contributions of this study are as follows:

- We propose a deep CNN that can classify 4-classes of disease stages in AD.
- The proposed hybrid model demonstrates superior performance for AD diagnosis from an imbalanced dataset and a small number of features.
- The manual feature extraction task of radiologists is eliminated with the developed hybrid CNN model.

The highlights of this study are as follows:

- 4-class brain MRI images are classified using 10 CNN architectures.
- The model proposed in this study aims to improve classification performance in AD diagnosis.
- Different feature maps of the 3 best CNN architectures are concatenated with Grad-CAM features.
- Thanks to this method, different features of the same images obtained in three different architectures are brought together.
- NCA dimension reduction is applied to the feature map to improve model performance.
- Obtained feature map is classified over 3 different ML classifiers.
- High-accuracy classification has been made for 4-class dementia stages of AD.
- As a result, in the proposed method, feature extraction, feature combining, dimension reduction and classification of the obtained feature map in three different classifiers were performed.

The rest of the article is as follows: Section 2 covers related works in the field of diagnosis of AD. A full description of the proposed methodology is given in section 3. The experimental results obtained from our proposed hybrid CNN model and their comparison with existing methods are given in section 4. In section 5, the proposed method is thoroughly explored and contrasted with existing studies in the literature. Finally, section 6 describes the final result emphasizing the developed method.

2. Related Works

In this section, information about the current studies in the literature closest to the method proposed in our article for the detection of AD is given.

Hemanth et al. proposed two new neural networks, Modified Counter Propagation Neural Network (MCPN) and Modified Kohonen Neural Network (MKNN), to achieve a high convergence rate and accuracy. Changes have been made to the training methodologies of traditional CPN and Kohonen networks for the design of these networks. They used a dataset of 540 MRI images to evaluate the performance of the proposed method. When the test results were examined, it was seen that the two proposed new methods, MKNN and MCPN, were 95% and 98% accurate, respectively [16].

Liu et al. used Densenet as a model for the Alzheimer's dataset, which consists of three classes. Softmax was employed as the classification layer in this investigation, and the accuracy rate was 88.9% [17].

Ahmed et al. used visual features from the hippocampal area, the region most affected by AD, to automatically classify AD from MRI images. Using Circulars Harmonic Functions from the hippocampal region, they extracted two types of features: visual local identifiers and the amount of BOS pixels in this area. In addition, a late fusion was used to achieve successful results. They used two datasets, ADNI and Bordeaux, to evaluate the effectiveness of their proposed method. In these two datasets, the accuracy values obtained for AD and Normal Control (NC) subjects are 87% and 85%. In the ADNI dataset, the accuracy values obtained for MCI vs. NC and MCI vs. AD were 78.22% and 72.23%, respectively, in subjects with Mild Cognitive Impairment (MCI) [18].

In this study, the gray matter section of T1-weighted MR images from cognitively normal older people with pathologically confirmed AD was classified using linear support vector machines [19].

In addition, Farooq et al. tested the performance of their proposed method for detecting AD with brain MRI images consisting of 4 classes. The researchers divided the MRI images in the dataset into 4 different groups in order to detect the disease more easily. They also applied some preprocessing to their data. Researchers used Googlenet, Resnet18, and Resnet152 architectures in their proposed method, and the highest accuracy rate was 98.88% with GoogleNet architecture [20].

Jongkreangkrai et al. combined the hippocampus and amygdala volumes and entorhinal cortex thickness in their proposed method to diagnose AD. Hippocampus, amygdala, and entorhinal cortex thickness in both cerebral hemispheres were measured using T1-weighted MR images of 100 Alzheimer's patients and 100 healthy individuals. Next, 5 different combinations of these features were used to compare the performance of the SVM algorithm for the classification of AD [21].

Moradi et al. proposed a two-step method for estimating conversion from mild cognitive impairment to AD from MRI images. In the first step of the method, they performed a feature selection process for the selection of Alzheimer's-related voxels in MRI images. They then used ML algorithms to predict the transition from mild cognitive impairment to AD [22].

In a different study, an automated-based method using 3D-CNN and SVM was proposed for AD. The researchers compared it with the 2D-CNN structure to test the effectiveness of the proposed method. An accuracy rate of 96.82% was obtained with this method for the automatic diagnosis of AD [23].

In a different study, the effect of measurements of cortical thickness on the detection of AD was investigated. For this purpose, the effectiveness of the suggested method was assessed on 19 patients and 17 healthy people [24].

Cheng et al. proposed a two-step Multi-Domain Transfer Learning method for AD. In the first step of the method, multi-domain transfer feature selection was made. In this step, the most relevant features for the diagnosis of AD were selected from the multi-domain data. In the second step of the method, they performed multi-domain transfer classification for the early diagnosis of AD. They evaluated the performance of their suggested technique using MRI images from 807 participants in the ADNI dataset [25].

Sarraf and Tofighi proposed a method using one of the CNN architectures, LeNet5, for AD using brain MRI. The accuracy value obtained with this method using cloud computing is 96.85% [26].

Billones et al. proposed a method using CNN for the detection of AD and MCI. In this method, they used 16-layer VGGNet. They obtained an accuracy of 91.85% from their method, which they tested on 20 randomly selected MRI images from each subject [27].

Khagi and Kwon proposed a CNN-based model for the diagnosis of AD. The researchers used brain MRI and PET images, consisting of 3 classes of 122 images, to test the effectiveness of their proposed method. This CNN-based method, which combines characteristic information, has an accuracy of 96% [28].

In a different study, a model combining sparse autoencoders and convolutional neural networks is proposed for the diagnosis of AD. In the proposed method, sparse autoencoders are first trained on randomly selected 3D brain MRI images. In this way, they learned filters for convolution operations. Then, a 3D CNN design was made with the learned filters [29]. Similarly, in a different study proposed for the diagnosis of AD, a 3D-CNN model that can learn AD-related features is proposed. This method is designed on a pre-trained 3D convolutional autoencoder. Researchers evaluated the effectiveness of the method in the ADNI and CADDementia datasets [30].

Alzheimer's was diagnosed in another study using SVM, IVM, and RELM algorithms on a 2-class MRI dataset [31]. The RELM algorithm gave better results than other algorithms with a 76.61% accuracy rate using 10 times cross-entropy. In this method proposed by Lama et al., the accuracy rates obtained with SVM and IVM algorithms are 75.33% and 60.2%, respectively.

Hon and Khan, on the other hand, proposed a model for Alzheimer's detection using VGG and Inception V4 architectures. They initialized these architectures using pre-trained weights from large benchmark datasets. Image entropy is used instead of randomly selecting training slices. The experimental evaluation of the proposed method was made on the OASIS dataset and the Inception V4 architecture achieved 96.25% accuracy [32].

Oh et al. proposed a method using autoencoder and 3D-CNN to detect AD. In the proposed method, data preprocessing (reorganization, normalization, smoothing), segmentation, and feature extraction steps are performed respectively. The researchers tested the performance of their proposed method on the ADNI dataset and obtained an accuracy value of 84.5% [33].

In their study, Eroglu et al. proposed a hybrid architecture using MRI in Darknet53, InceptionV3, and Resnet101 models to classify different levels of AD. In the proposed architecture, Alzheimer's brain MR images were classified with SVM and KNN classifiers, and they achieved 99.1% accuracy [34].

In comparison to other research in the literature, the hybrid model we proposed in this study produced better outcomes. The model we proposed allowed for the combination of various features of the same image by employing three different architectures as its foundation, extracting features, and merging these features. The developed model was then applied to create quicker and more successful results using the NCA approach. In order to determine which ML classifiers the proposed model would perform better in, three distinct classifiers were utilized.

3. Materials and Methods

This section describe the proposed hybrid model, analyzes the dataset of the study and Grad-CAM Heatmap visualization, the DL architectures used for feature extraction, and the NCA approach used for feature selection.

3.1. Proposed Hybrid Model

A combination of the best 3 architectures DenseNet201, EfficientNet-B0 and AlexNet architectures from 10 pre-trained CNN architectures was used for the proposed hybrid method. A total of 6400×3000 features were obtained, 1000 features from the FC layer of each architecture. In addition to the original dataset, feature extraction with these 3 architectures was also applied to the Grad-CAM visualization results that highlight the tissue features of each brain MR image. Then, this feature matrix with the size of 6400×6000 is reduced by the NCA feature selection method. While the feature numbers of the optimized features in this step remained the same, the total number of features was reduced to 400. Thus, the feature matrix of 6400×400 size, selected among the most ideal features, was classified separately in the ML classifiers KNN, Ensemble, and SVM. The workflow of this proposed hybrid model is illustrated in Fig 2.

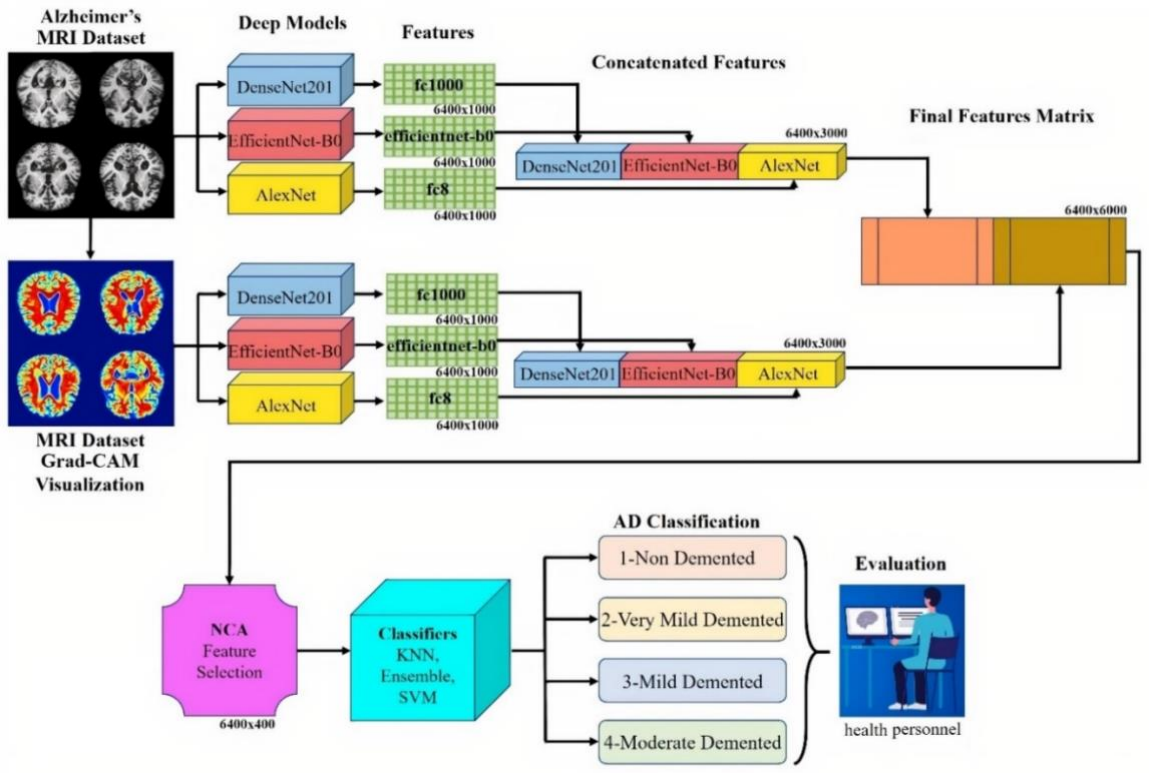

Figure 2. The flow chart of the proposed hybrid method

Using the proposed hybrid model, AD was classified in 4-levels in KNN, Ensemble, and SVM classifiers, and these images were presented to the expert.

3.2. Brain MRI Dataset Description

The dataset consists of 6400 brain MRI images in total, which were evaluated in 4 different stages of AD: Non Demented, Very Mild Demented, Mild Demented, and Moderate Demented. Data was collected from various web sources, each with a verified tag. The dataset is a publicly available dataset divided into two subfolders, test and train [35]. In Table 1, the data numbers for each folder are listed. The images in the dataset are in .jpg format. Since they are 8-bit deep, the images have been converted to 24-bit.

Table 1. Image counts of the brain MRI dataset

Dataset	Non Demented	Very Mild Demented	Mild Demented	Moderate Demented	Total
Train	2560	1792	717	52	5121
Test	640	448	179	12	1279
Total	3200	2240	896	64	6400

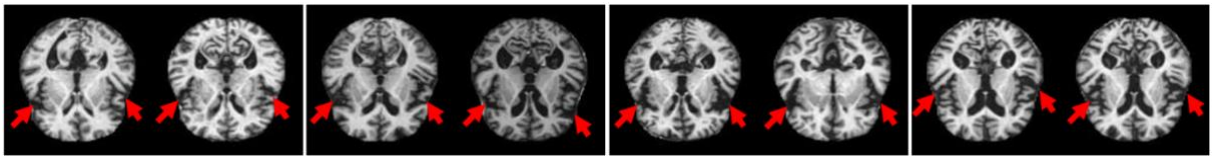

Figure 3. Samples of the brain MRI dataset

Fig 3 presents samples of the four classes in the dataset in groups of two. In the samples of the brain MRI dataset, atrophy of the temporal lobe of the brain and subarachnoid spaces are shown in groups of 2 at 4 stages with red arrows.

3.3. Grad-CAM Visualization

Grad-CAM is a well-liked method for displaying the search space of a CNN model. Grad-CAM can provide a unique visualization for each class that is present in the image because it is class-specific. Grad-CAM is the process of finding particular objects using a model that was trained using whole-image labels instead of explicit position annotations which can be used for weakly-supervised localization. Grad-CAM can be used to shed more light on a model's shortcomings, such as the reasons why a model failed [36].

The class activation mapping (CAM) method has been generalized as Grad-CAM. The gradients of the classification score with respect to the finished convolutional feature map are used in the Grad-CAM interpretability technique. The portions of a picture that have a significant value on the Grad-CAM map are those that have the most effects on the network score for that class [37].

The pioneering innovations of Grad-CAM and the main advantages of using it for this study are listed as follows:

- Based on a specified input image, a trained CNN, and a selected class of interest, Grad-CAM is a popular method for producing a class-specific Heatmap.
- Grad-CAM can be computed on any CNN architecture as long as the layers are differentiable.
- Weakly supervised segmentation and localization have both been accomplished using Grad-CAM.

Deeper representations in a CNN are said to capture higher-level visual structures, according to a number of earlier works [38]. Grad-CAM assigns appropriate values to each neuron for a given decision of interest using the gradient data entering the last convolutional layer of the CNN [39]. Our method combines feature maps from several DL architectures with results from Grad-CAM in order to explain output layer decisions.

According to task-specific computations of Grad-CAM as given in Eq. 1. First of all, the gradient of the score for the c class must be calculated, y^c (before the softmax), with respect to the feature map activations A^k of a convolutional layer in order to create the class-discriminative localization map Grad-CAM $L^c_{Grad-CAM} \in \mathrm{R}^{uxv}$ of width u and height v for any class c, i.e. $\frac{\partial y^c}{\partial A^k}$. These gradients flowing back are global-average-pooled throughout the width and height dimensions to produce the neuron significance weights α^c_k (indexed by i and j, respectively):

$$\alpha_k^c = \overbrace{\frac{1}{Z}\sum_i\sum_j}^{\text{global average pooling}} \underbrace{\frac{\partial y^c}{\partial A_{ij}^k}}_{\text{gradients via backprop}} \tag{1}$$

Up until the last convolution layer to which the gradients are being propagated, the actual computation for computing α^c_k while backpropagation gradients with respect to activations. Which consist of the weight matrices and gradient with regard to activation functions' successive matrix products. As a result, this weight α^c_k denotes a partial linearization of the deep network downstream from A and captures the "importance" of feature map k for a target class c. In Eq. 2 to get, we combine forwarding activation maps in a weighted manner with a ReLU.

$$L^c_{Grad-CAM} = ReLU \underbrace{\left(\sum_k \alpha_k^c A^k\right)}_{\text{linear combination}} \tag{2}$$

In the final convolutional layers of GoogleNet, this produces a coarse Heatmap that is the same size as the convolutional feature maps. Since we are only interested in characteristics that positively affect the class of interest, we apply a ReLU to the linear combination of maps. i.e., pixels whose intensity should be increased to improve y^c. Negative pixels are probably part of other image types. Localization maps frequently highlight classes other than the one intended and perform less well in terms of localization without this ReLU. In the samples of the brain MRI dataset, atrophy of the temporal lobe of the brain and subarachnoid spaces are shown in groups of 2 at 4 stages within red and blue tones using Grad-CAM. 2 samples of 4 stages are shown in Fig 4. In general, a CNN image classification class score does not have to be y^c. Any distinguishable activation, such as words from a caption or a response to a query, is possible. The first group stage to the fourth group stage with red-blue coloration distinguishes the disease by temporal lobe atrophy and subsequent dilatations in the subarachnoid spaces.

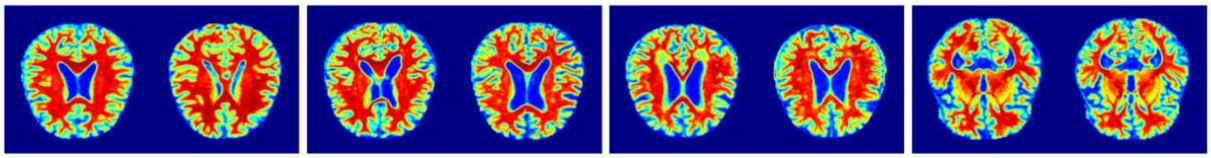

Figure 4. Samples from Grad-CAM results of brain MRI dataset

3.4. Pre-trained CNN Architectures

Table 2. Brain MRI dataset classification results (accuracy %) of 10 CNN architectures

Models	KNN	Models	Ensemble	Models	SVM
DenseNet201	98.5	DenseNet201	98.3	EfficientNet-B0	94.5
EfficientNet-B0	98.4	EfficientNet-B0	97.9	AlexNet	93.1
AlexNet	97.9	MobileNetV2	97.2	DenseNet201	92.9
MobileNetV2	97.9	AlexNet	97.1	ResNet101	90.3
ShuffleNet	97.4	ShuffleNet	96.6	ShuffleNet	89.5
VGG19	96.4	VGG19	96.0	MobileNetV2	89.3
DarkNet53	96.3	DarkNet53	95.7	DarkNet53	88.7
ResNet101	95.7	ResNet101	94.9	VGG19	88.0
InceptionV3	94.0	InceptionV3	93.3	InceptionV3	86.3
GoogleNet	91.0	GoogleNet	89.7	GoogleNet	83.2

According to the order given in Table 2, DenseNet201 [40], EfficientNet-B0 [41], and AlexNet [42] architectures, which show high performance using KNN, Ensemble, and SVM classifiers, were preferred for feature concatenation.

The underlying principle is to move the filters over the image to generate the features of the inputs. These filters applied to the inputs or to each convolution layer may differ in each model [43]. Eq. 3 is used to determine the size of the output image after the convolution layer's image filtering.

$$o = ((i - k) + 2p)/s + 1 \tag{3}$$

here, o, i, and k represent output, input, and filter size, respectively. p and s represent padding and step count, respectively. The convolution operation is performed with Eq. 4.

$$S(i,j) = (I * K)(i,j) = \sum_m \sum_n I(m,n)K(i-m, j-n) \tag{4}$$

here, I, S, and K represent input, output, and kernel, respectively.

The activation function is another component of CNN models. Here, many activation functions may be preferred. The following Eq. 5-7 provide the most popular activation functions [44].

$$ReLU: f(x) = \begin{cases} 0, x < 0 \\ x, x \geq 0 \end{cases}, f(x)' = \begin{cases} 0, x < 0 \\ 1, x \geq 0 \end{cases} \tag{5}$$

$$Sigmoid: f(x) = \frac{1}{1+e^{-x}}, f(x)' = f(x)(1-f(x)) \tag{6}$$

$$Tanh: tanh(x) = \frac{2}{1+e^{-2x}} - 1, f(x)' = 1 - f(x)^2 \tag{7}$$

Normalization is another feature of CNN models. The effectiveness of the architecture may be impacted by this procedure. Eq. 8-10 are described the normalizing procedure [45].

$$Y_i = \frac{X_i - \mu_\beta}{\sqrt{\sigma_\beta^2 + \epsilon}} \tag{8}$$

$$\sigma_\beta = \frac{1}{M}\sum_{i=1}^{M}(X_i - \mu_\beta)^2 \tag{9}$$

$$\mu_\beta = \frac{1}{M}\sum_{i=1}^{M} X_i \tag{10}$$

here, Y_i is the value following normalization. σ_β is the standard deviation. μ_β represents the average value, M represents the number of input.

3.5. NCA-Feature Selection

The non-parametric method of NCA is used to select features. The main aim is to increase the accuracy of regression and classification algorithms' predictions. The basic formulations of the algorithm are listed as follows;

Assuming $T = \{(x_1, y_1), \ldots, (x_i, y_i), \ldots, (x_N, y_N)\}$ is the set of training samples, x_i represents the d-dimensional feature vector, $y_i \in \{1, \ldots, C\}$ its associated class label, and N the number of instances. The purpose is to find a weighting vector w that allows for feature subset selection and nearest neighbor classification optimization. The weighted distance between two samples x_i and x_j is expressed in terms of the weighting vector w as shown in Eq. 11:

$$d_w(x_i, x_j) = \sum_{r=1}^{d} w_r^2 \left|x_{ir} - x_{jr}\right|, \tag{11}$$

where w_r denotes the weight of the rth feature. Optimizing its leave-one-out classification accuracy on the training set T is a simple and efficient method for closest neighbor classification success. Since the actual leave-one-out accuracy used to select the nearest neighbor as a classification reference point is a non-differentiable function, a probability distribution is utilized as an efficient approximation. The probability that x_i selects x_j as its reference point is given by Eq. 12;

$$p_{ij} = \begin{cases} \frac{\kappa\left(d_w(x_i, x_j)\right)}{\sum_{k \neq i} \kappa\left(d_w(x_i, x_k)\right)}, & \text{if } i \neq j \\ 0, & \text{if } i = j \end{cases} \tag{12}$$

The kernel width σ is an input parameter that controls the likelihood of specific points being chosen as the reference point when kernel function $\kappa(z) = \exp(-z/\sigma)$is applied. In specifically, only the query sample's closest neighbor can be chosen as its reference point, if $\sigma \to 0$. While all the points aside from the question point have the same chance of getting chosen, if $\sigma \to +\infty$. According to the definition above, the likelihood that query point x_i will be successfully categorized is given in Eq. 13:

$$p_i = \sum_j y_{i\,j}\, p_{i\,j} \tag{13}$$

here $y_{ij} = 1$ if and only if $y_i = y_j$ and otherwise $y_{ij} = 0$. Thus, the approximate leave-one-out classification accuracy is represented by Eq. 14:

$$\xi(w) = \frac{1}{N}\sum_i p_i = \frac{1}{N}\sum_i \sum_j y_{i\,j}\, p_{i\,j} \tag{14}$$

$\xi(w)$ is represents the true genuine leave-one-out classification accuracy while $\sigma \to 0$. We also include a regularization term to do feature selection and reduce overfitting, and as a result, we get the objective function shown in Eq. 15:

$$\xi(w) = \sum_i \sum_j y_{i\,j}\, p_{i\,j} - \lambda \sum_{r=1}^{d} w_r^2 \tag{15}$$

where the cross-validation method can be used to adjust the regularization parameter $\lambda > 0$. The coefficient $1/N$ in Eq. 14 is ignored, as it just indicates that the parameter λ changes in accordance with the equation, leaving the final solution vector unchanged. The derivative with respect to w_r of the object function $\xi(w)$ can be calculated in Eq. 16 because it is differentiable:

$$\begin{aligned}\frac{\partial \xi(w)}{\partial w_r} &= \sum_i \sum_j y_{i\,j} \left[\frac{2}{\sigma}\; p_{i\,j} \left(\sum_{k\neq i} p_{i\,k}\, |x_{i\,r} - x_{k\,r}| - |x_{i\,r} - x_{j\,r}|\right) w_r\right] - 2\lambda w_r \\ &= \frac{2}{\sigma}\sum_i \left(p_i \sum_{k\neq i} p_{i\,k}\, |x_{i\,r} - x_{k\,r}| - \sum_j y_{i\,j}\, p_{i\,j}\, |x_{i\,r} - x_{j\,r}|\right) w_r - 2\lambda w_r \\ &= 2\left(\frac{1}{\sigma}\sum_i \left(p_i \sum_{j\neq i} p_{i\,j}\, |x_{i\,r} - x_{j\,r}| - \sum_j y_{i\,j}\, p_{i\,j}\, |x_{i\,r} - x_{j\,r}|\right) - \lambda\right) w_r\end{aligned} \tag{16}$$

The relevant gradient ascent update equation can be acquired by using the aforementioned derivative. The suggested approach is known as NCA-FS [46]. It should be observed that we skipped the line search procedure in the iteration to determine the step length α. The evaluation of the goal function necessitates expensive calculation, which is the fundamental cause.

4. Experimental Results

The features obtained using DenseNet201, EfficientNet-B0 and AlexNet architectures were concatenated and classified by KNN, Ensemble and SVM ML algorithms. Moreover, in order to emphasize the contribution of Grad-CAM visualization, which is a part of the proposed hybrid model, to the experimental results, the feature extraction classification results of the hybrid model without Grad-CAM are included. Finally, the experimental results, confusion matrices, and performance metrics obtained from the proposed hybrid model are given.

Table 3. Parameter values used in training

Environment	Max Epoch	Learning Rate	Mini batch size	Optimization
Matlab R2021b	5	1e-4	32	Sgdm

All applications were executed in MATLAB R2021b environment and on a machine includes a GTX 1080 graphics card and 16 GB of RAM. In order to compare the outcomes reliably, the same parameters were applied during the training of these pre-trained deep architectures. The learning parameters are illustrated in Table 3.

Default values are used in these ML classifiers. CNN models convert different sizes of input images to a standard size. The input image sizes of DenseNet201, EfficientNet-B0, and AlexNet CNN architectures are 224×224, 224×224, and 227×227, respectively. The dimensions of the input images of the architectures used were adjusted to the dimensions specified before the training.

The initial value of the KNN classifier, which is one of the preferred classifiers in the study, is fine KNN. The number of neighbors is given as 1. The distance measure was chosen as Euclidean. The 5-fold is determined in the KNN algorithm. The Ensemble classifier is another algorithm used in the study. The kernel function of this classifier is a subset of KNN. Another classifier in the study is the SVM classifier. Cubic SVM is the kernel function. The core scale value is automatically selected and the cost matrix is the default. As in KNN, the 5-fold is also determined in SVM. In the confusion matrix, it represents the 1st class Non Demented stage, the 2nd class Very Mild Demented stage, the 3rd class Mild Demented stage, and the 4th class Moderate Demented stage.

4.1. Performance metrics

In this study, six different performance evaluation criteria are used to evaluate and compare the proposed method: accuracy, sensitivity, specificity, precision, F1-measure, and Matthews Correlation Coefficient (MCC). These TP, TN, FP, and FN metrics in Table 4 represent true positive, true negative, false positive, and false negative, respectively.

Table 4. Statistical performance metrics of the CNN architectures

		Predicted Class	
		Positive	**Negative**
True Class	**Positive**	True Positive (***TP***)	False Negative (***FN***)
	Negative	False Positive (***FP***)	True Negative (***TN***)

$$Accuracy = \frac{\mathrm{TP} + \mathrm{TN}}{\mathrm{TP} + \mathrm{TN} + \mathrm{FP} + \mathrm{FN}} \tag{17}$$

$$Sensitivity = \frac{\mathrm{TP}}{\mathrm{TP} + \mathrm{FN}} \tag{18}$$

$$Specificity = \frac{\mathrm{TN}}{\mathrm{TN} + \mathrm{FP}} \tag{19}$$

$$Precision = \frac{\mathrm{TP}}{\mathrm{TP} + \mathrm{FP}} \tag{20}$$

$$F1 - measure = \frac{2\ \mathrm{TP}}{(2\ \mathrm{TP} + \mathrm{FP} + \mathrm{FN})} \tag{21}$$

$$MCC = \frac{(\mathrm{TP} * \mathrm{TN}) - (\mathrm{FP} * \mathrm{FN})}{\sqrt{((\mathrm{TP} + \mathrm{FP}) * (\mathrm{TP} + \mathrm{FN}) * (\mathrm{TN} + \mathrm{FP}) * (\mathrm{TN} + \mathrm{FN}))}} \tag{22}$$

4.2. DenseNet201

The fc1000 layer of the DenseNet201 architecture was used to extract features from images in the Alzheimer's brain MRI dataset. These obtained features were classified through KNN, Ensemble, and SVM algorithms. Table 5 illustrates every confusion matrix produced by the classifier algorithms.

Each of the KNN, Ensemble, and SVM algorithms separately classified the features extracted from the DenseNet201 model. The accuracy values obtained from the KNN, Ensemble, and SVM algorithms are 98.5%, 98.3%, and 92.9%, respectively. When the results are examined, it is seen that the KNN algorithm is more successful than other algorithms in classifying the features extracted from the DenseNet201 model. The KNN

algorithms accurately predicted 3161 of 3200 Non Demented images, 2201 of 2240 Very Mild Demented images, 878 of 896 Mild Demented images, and 62 of 64 Moderate Demented images. Thus, the DenseNet201 architecture predicted 6302 correctly and 98 incorrectly out of a total of 6400 images. In this architecture, although the accuracy value of the Ensemble classifier is more successful than the SVM classifier, these two architectures lagged behind the KNN classifier.

Table 5. Confusion matrix obtained from DenseNet201, EfficientNet-B0, and AlexNet

DenseNet201+KNN (98.5%)					
True class	**1**	3161	26	12	1
	2	30	2201	9	
	3	3	14	878	1
	4	1	1		62
		1	**2**	**3**	**4**
		Predicted class			

DenseNet201+Ensemble (98.3%)					
True class	**1**	3160	27	12	1
	2	32	2197	11	
	3	5	15	875	1
	4	2	1		61
		1	**2**	**3**	**4**
		Predicted class			

DenseNet201+SVM (92.9%)					
True class	**1**	3050	121	29	
	2	161	2056	23	
	3	37	65	794	
	4	2	14	1	47
		1	**2**	**3**	**4**
		Predicted class			

EfficientNet+KNN (98.4%)					
True class	**1**	3150	45	5	
	2	28	2203	9	
	3	6	10	879	1
	4				64
		1	**2**	**3**	**4**
		Predicted class			

EfficientNet+Ensemble (97.9%)					
True class	**1**	3141	47	11	1
	2	37	2191	12	
	3	10	12	873	1
	4			1	63
		1	**2**	**3**	**4**
		Predicted class			

EfficientNet+SVM (94.5%)					
True class	**1**	3077	113	9	1
	2	121	2101	18	
	3	39	40	816	1
	4		7		57
		1	**2**	**3**	**4**
		Predicted class			

AlexNet+KNN (97.9%)					
True class	**1**	3146	44	9	1
	2	35	2192	12	1
	3	17	16	863	
	4		1		63
		1	**2**	**3**	**4**
		Predicted class			

AlexNet+Ensemble (97.1%)					
True class	**1**	3129	55	15	1
	2	48	2171	18	3
	3	23	21	851	1
	4		1	1	62
		1	**2**	**3**	**4**
		Predicted class			

AlexNet+SVM (93.1%)					
True class	**1**	3057	123	20	
	2	153	2064	23	
	3	46	69	781	
	4	2	5	1	56
		1	**2**	**3**	**4**
		Predicted class			

4.3. EfficientNet-B0

The efficientnet-b0|model|dense|Matmul layer of the EfficientNet-B0 architecture was used to extract features from images in the Alzheimer's brain MRI dataset. These obtained features were classified through KNN, Ensemble, and SVM algorithms. Table 5 illustrates every confusion matrix produced by the classifier algorithms.

Each of the KNN, Ensemble, and SVM algorithms separately classified the features extracted from the EfficientNet-B0 model. The accuracy values obtained from the KNN, Ensemble, and SVM algorithms are 98.4%, 97.9%, and 94.5%, respectively. When the results are examined, it is seen that the KNN algorithm is more successful than other algorithms in classifying the features extracted from the EfficientNet-B0 model. The KNN algorithms accurately predicted 3150 of 3200 Non Demented images, 2203 of 2240 Very Mild Demented images, 879 of 896 Mild Demented images, and 64 of 64 Moderate Demented images. Thus, the EfficientNet-B0 architecture predicted 6296 correctly and 104 incorrectly out of a total of 6400 images. In this architecture, although the accuracy value of the Ensemble classifier is more successful than the SVM classifier, these two architectures lagged behind the KNN classifier.

4.4. AlexNet

The fc8 layer of the AlexNet architecture was used to extract features from images in the Alzheimer's brain MRI dataset. These obtained features were classified through KNN, Ensemble, and SVM algorithms. Table 5 illustrates every confusion matrix produced by the classifier algorithms.

Each of the KNN, Ensemble, and SVM algorithms separately classified the features extracted from the AlexNet model. The accuracy values obtained from the KNN, Ensemble, and SVM algorithms are97.9%, 97.1%, and 93.1%, respectively. When the results are examined, it is seen that the KNN algorithm is more successful than other algorithms in classifying the features extracted from the AlexNet model. The KNN algorithms accurately predicted 3146 of 3200 Non Demented images, 2192 of 2240 Very Mild Demented images, 863 of 896 Mild Demented images, and 63 of 64 Moderate Demented images. Thus, the AlexNet architecture predicted 6264 correctly and 136 incorrectly out of a total of 6400 images. In this architecture, although the accuracy value of the

Ensemble classifier is more successful than the SVM classifier, these two architectures lagged behind the KNN classifier.

4.5. Proposed NCA-Based Hybrid Model

Features from DenseNet201, EfficientNet-B0, and AlexNet architectures are concatenated without Grad-CAM. Thus, a feature matrix with a total size of 6400×3000 was produced. NCA feature selection was used to optimize this matrix and the matrix size was reduced to 6400×400. Then the reduced features were classified with KNN, Ensemble, and SVM classifiers. Table 6 shows the confusion matrices from this process obtained proposed hybrid model without Grad-CAM. Fig 5 shows best result AUC curves for each class of AD with the proposed hybrid model + KNN classifers.

Table 6. Confusion matrix obtained from the proposed hybrid model

Hybrid model+KNN (99.5%)					
True class	**1**	3193	4	2	1
	2	12	2226	2	
	3	2	5	889	
	4	1			63
		1	**2**	**3**	**4**
		Predicted class			

Hybrid model+Ensemble(99.4%)					
True class	**1**	3188	9	2	1
	2	12	2226	2	
	3	5	5	886	
	4	1	1		62
		1	**2**	**3**	**4**
		Predicted class			

Hybrid model+SVM (97.5%)					
True class	**1**	3155	34	11	
	2	58	2173	9	
	3	13	30	853	
	4	2	5		57
		1	**2**	**3**	**4**
		Predicted class			

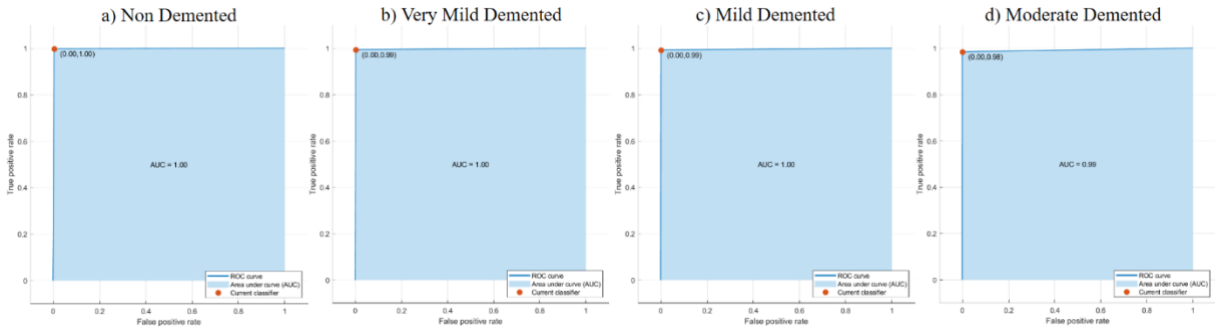

Figure 5. Hybrid model + KNN AUC curves of four class AD.

In the proposed hybrid model, in addition to 6400×3000 features obtained from DenseNet201, EfficientNet-B0, and AlexNet architectures, Grad-CAM visualization results obtained from each image of the dataset are given for feature extraction to these architectures. Thus, a total of 6400×6000 size feature matrix was created by adding the 6400×3000 size feature matrix obtained from Grad-CAM to the 6400×3000 size feature matrix obtained from the original dataset. To optimize this matrix, NCA feature selection was used again and the matrix size was reduced to 6400×400. Then the reduced features were classified with KNN, Ensemble, and SVM. Table 7 shows the confusion matrices from this process obtained proposed hybrid model using Grad-CAM. Fig 6 shows best result AUC curves for each class of AD with the proposed hybrid model + Ensemble classifers.

Table 7. Confusion matrix obtained from the proposed hybrid model using Grad-CAM

Hybrid model+Ensemble(99.83%)					
True class	**1**	3195	5		
	2	4	2236		
	3	2	1	893	
	4				64
		1	**2**	**3**	**4**
		Predicted class			

Hybrid model+KNN (99.7%)					
True class	**1**	3191	8	1	
	2	4	2234	2	
	3	1	1	894	
	4				64
		1	**2**	**3**	**4**
		Predicted class			

Hybrid model+SVM (97.5%)					
True class	**1**	3154	41	5	
	2	62	2171	7	
	3	22	20	854	
	4		2	2	60
		1	**2**	**3**	**4**
		Predicted class			

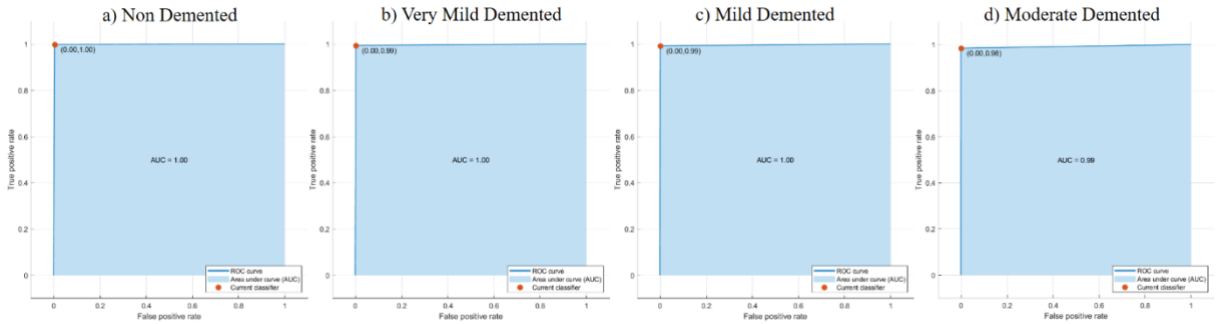

Figure 6. Hybrid model + Ensemble AUC curves of four class AD using Grad-CAM.

When the experimental results in Table 6 are examined, the accuracy values obtained from the KNN, Ensemble, and SVM classifiers are 99.5%, 99.4%, and 97.5%, respectively. KNN classifier was more successful than Ensemble and SVM in this hybrid model made on the original dataset without Grad-CAM. This KNN classifier algorithm accurately predicted 3193 of 3200 Non Demented images, 2226 of 2240 Very Mild Demented images, 889 of 896 Mild Demented images, and 63 of 64 Moderate Demented images. Thus, the NCA-based hybrid model without Grad-CAM predicted 6371 correctly and 29 incorrectly out of a total of 6400 images.

When the experimental results in Table 7 are examined, the accuracy values obtained from Ensemble, KNN, and SVM classifiers are 99.83%, 99.7%, and 97.5%, respectively. In this proposed hybrid model, implemented using Grad-CAM with the original dataset, the Ensemble classifier was more successful than KNN and SVM. This Ensemble classifier algorithm accurately predicted 3195 of 3200 Non Demented images, 2236 of 2240 Very Mild Demented images, 893 of 896 Mild Demented images, and 64 of 64 Moderate Demented images. Thus, the NCA-based hybrid model with Grad-CAM predicted 6388 correctly and 12 incorrectly out of a total of 6400 images.

The overall performance rate of the proposed hybrid model 99.83% accuracy, 99.88% sensitivity, 99.92% specificity, 99.83% precision, 99.85% F1-measure, and 99.78% MCC results using the Ensemble classifier for the 4-class classification of AD. Table 8 provides an evaluation of the proposed hybrid model + Ensemble performance using Grad-CAM visualization.

Table 8. The 4-class performance results of the proposed hybrid model + Grad-CAM + Ensemble(%)

AD	Stage	Accuracy	Sensitivity	Specificity	Precision	F1	MCC
Proposed hybrid model + Grad-CAM + Ensemble	NonDemented	99.84	99.81	99.84	99.84	99.82	99.65
	VeryMildDemented	99.82	99.73	99.90	99.82	99.77	99.65
	MildDemented	99.66	1	99.94	99.66	99.83	99.80
	ModerateDemented	1	1	1	1	1	1
	Overall	99.83	99.88	99.92	99.83	99.85	99.78

5. Discussion

The neurodegenerative brain disorder AD gets worse over time. Increased Amyloid-β level causes oxidative damage in brain cells. In this case, the cognitive decline seen in AD has been associated with it. AD is highly correlated with the age factor and its incidence is higher in advancing ages. In the future, Alzheimer's patient numbers are anticipated to rise, particularly in industrialized nations, as the percentage of elderly people in the population grows [47]. The prevention or delay of the disease's progression, as well as the ease of the disease's monitoring depend on an early diagnosis of Alzheimer's. Imaging techniques are one of the most used ways to diagnose AD [48, 49]. Imaging techniques can also disable other factors of this disease. Specific findings on MRI are used to diagnose AD [50]. Although it is not used frequently today, there are many works using MR methods for the diagnosis and follow-up of AD. These are; Diffusion Tensor Imaging (DTI), functional MRI, and Magnetic Resonance Spectroscopy (MRS) [51-53]. In AD, brain MRI shows temporoparietal lobe atrophy predominantly in the mesial temporal region. With disease progression, more atrophy affects areas close to the temporal region. Mesial temporal lobe atrophy causes a reduction in the hippocampus and parahippocampus volume and enlargement of the parahippocampal fissure. Parietal atrophy occurs in the early stages of the disease.

Today, artificial intelligence and machine learning techniques are used by many researchers in different subjects such as biomedical image processing, text, and voice analysis [54-56]. In this study, a method is proposed

to diagnose AD, which negatively affects the quality of life, according to the severity of dementia using Alzheimer's MRIs. Early diagnosis of the disease may be delayed due to the difficulty of interpreting Alzheimer's MRIs. These delays in the diagnosis of the disease cause delays in treatment as well as cause irreversible problems. In this study, AD was divided into 4 different classes using a ML-based model on brain MRI images. In the first step of the proposed method, feature extraction was performed from brain MRI images using DenseNet201, EfficientNet-B0, and AlexNet CNN architectures. Then, Grad-CAM visualization was applied to the entire AD MRI dataset, which clearly revealed the enlargement of the parahippocampal fissure due to the reduction in the volume of the hippocampus and parahippocampus. The same 3 CNN architectures were applied to the obtained Grad-CAM images for feature extraction. Next, all the features from these 3 different architectures applied to both the AD MRI dataset and the Grad-CAM visualization were combined. The NCA approach was used to optimize all of these combined features. Then, these concatenated features were classified by KNN, Ensemble, and SVM ML algorithms. When Table 9 is examined, it is seen that the method proposed in this study is the most successful. CNN architectures used in this hybrid model, which uses DL CNN and ML methods together, have achieved more successful results than other methods in the literature.

Table 9. Accuracy (%) rates from different models

Models / Classifiers	KNN	Ensemble	SVM
DenseNet201	98.5%	98.3%	92.9%
EfficientNet-B0	98.4%	97.9%	94.5%
AlexNet	97.9%	97.1%	93.1%
Proposed hybrid method without Grad-CAM	99.5%	99.4%	97.5%
Proposed hybrid method using Grad-CAM	**99.7%**	**99.83%**	**97.5%**

Information on all available studies related to our study on AD are listed in Table 10. In Table 10, it is seen that the hybrid model proposed in this study gives higher results than other studies in the literature. According to the performance evaluation metrics in Table 4, the proposed model is an effective and usable method for AD diagnosis. Due to the disease's significant morbidity, accurate diagnosis is crucial. Thanks to this study, 4-stages of AD were diagnosed with high success using AD brain MRI images. According to the experimental results obtained, this method will contribute to the medical literature. The limitations of the proposed method are the lack of clinical data from patients.

Table 10. Comparison of similar studies in the literature

Study	Models/Methods	Accuracy (%)	Year
Lama et. al [31]	RELM	76.61	2017
Ahmed et. al [18]	SVM	78.22	2015
Oh et. al [33]	CNN	84.5	2019
Liu et. al [17]	DenseNet	88.9	2020
Klöppel et. al [19]	SVM	89.2	2008
Billones et. al [27]	VGGNet	91.85	2016
Hemanth et. al [16]	MKNN, MCPN	95, 98	2014
Khagi and Kwon [28]	CNN	96	2020
Hon and Khan [32]	VGG, Inception V4	96.25	2017
Feng et. al [23]	CNN+SVM	96.82	2020
Sarraf ve Tofighi [26]	LeNet5	96.85	2016
Farooq et. al [20]	GoogLeNet+ResNet18+ResNet152	98.88	2017
Eroglu et. al [34]	Darknet53+InceptionV3+Resnet101	99.1	2022
Odusami et. al [57]	ResNet18 + DenseNet201	98.86	2022
Razzak et. al [58]	PartialNet	99.26	2022
The proposed hybrid model without Grad-CAM	Densenet201+EfficientNet+AlexNet	**99.5**	2022
The proposed hybrid model using Grad-CAM	Densenet201+EfficientNet+AlexNet	**99.83**	2022

6. Conclusion

AD is a cause of dementia that is frequently seen in elderly individuals and negatively affects the families of the patients. Early diagnosis of Alzheimer's not only prevents the progression of the disease but also plays an important role in increasing the quality of life of patients. This disease is very difficult to diagnose, as the pixel density and images are similar in brain MRI of different individuals. The method in this study was proposed to diagnose AD using four-stage brain MRIs. The proposed method is a hybrid model using Grad-CAM to classify brain MRIs. The accuracy value obtained in this hybrid method using Grad-CAM to diagnose AD is 99.83%. The results obtained in this study were compared with the results of different studies on the subject in the literature. According to the comparison results, the proposed method is quite successful. The success of the results obtained with the proposed method shows that this method can facilitate the diagnosis of AD by experts and can alleviate their workload in this regard.

References

[1] Miller-Thomas, M. M., Sipe, A. L., Benzinger, T. L., McConathy, J., Connolly, S., & Schwetye, K. E. Multimodality review of amyloid-related diseases of the central nervous system. Radiographics 2016; 36(4): 1147.

[2] Qiu, C., Kivipelto, M., & Von Strauss, E. Epidemiology of Alzheimer's disease: occurrence, determinants, and strategies toward intervention. Dialogues Clin Neurosci, 2022.

[3] Jalbert, J. J., Daiello, L. A., & Lapane, K. L. Dementia of the Alzheimer type. Epidemiol Rev 2008; 30(1): 15-34.

[4] Altieri, M., Garramone, F., & Santangelo, G. Functional autonomy in dementia of the Alzheimer's type, mild cognitive impairment, and healthy aging: a meta-analysis. J Neurol Sci 2021; 42(5): 1773-1783.

[5] Fargo, K., & Bleiler, L. Alzheimer's association report: 2014 Alzheimers disease facts and figures. Alzheimers Dement 2014; 10(2): e47-e92.

[6] Bron, E. E., Smits, M., Van Der Flier, W. M., Vrenken, H., Barkhof, F., Scheltens, P., ... & Alzheimer's Disease Neuroimaging Initiative. Standardized evaluation of algorithms for computer-aided diagnosis of dementia based on structural MRI: the CADDementia challenge. NeuroImage 2015; 111: 562-579.

[7] Zuliani, G., Trentini, A., Rosta, V., Guerrini, R., Pacifico, S., Bonazzi, S., ... & Cervellati, C. Increased blood BACE1 activity as a potential common pathogenic factor of vascular dementia and late onset Alzheimer's disease. Sci Rep 2020; 10(1): 1-8.

[8] Norfray, J. F., & Provenzale, J. M. Alzheimer's disease: neuropathologic findings and recent advances in imaging. Am J Roentgenol 2004; 182(1): 3-13.

[9] Başkaya, O., Kandemir, M., Tepe, M. S., Acar, M., Ünal, G., Yalçıner, Z. B., & Ünay, D. Inter-hemispheric atrophy better correlates with expert ratings than hemispheric cortical atrophy. In 2012 20th Signal Processing and Communications Applications Conference (SIU), April 2012; (pp. 1-4). IEEE.

[10] Patel, K. P., Wymer, D. T., Bhatia, V. K., Duara, R., & Rajadhyaksha, C. D. Multimodality imaging of dementia: clinical importance and role of integrated anatomic and molecular imaging. Radiographics 2020; 40(1): 200.

[11] Lehmann, M., Koedam, E. L., Barnes, J., Bartlett, J. W., Ryan, N. S., Pijnenburg, Y. A., ... & Fox, N. C. Posterior cerebral atrophy in the absence of medial temporal lobe atrophy in pathologically-confirmed Alzheimer's disease. Neurobiol Aging 2012; 33(3): 627-e1.

[12] Sahiner, B., Chan, H. P., Petrick, N., Wei, D., Helvie, M. A., Adler, D. D., & Goodsitt, M. M. Classification of mass and normal breast tissue: a convolution neural network classifier with spatial domain and texture images. IEEE Trans Med Imaging 1996; 15(5): 598-610.

[13] Adem, K. Diagnosis of breast cancer with Stacked autoencoder and Subspace kNN. Phys. A: Stat. Mech. Appl. 2020; 551: 124591.

[14] Liu, M., Li, F., Yan, H., Wang, K., Ma, Y., Shen, L., ... & Alzheimer's Disease Neuroimaging Initiative. A multi-model deep convolutional neural network for automatic hippocampus segmentation and classification in Alzheimer's disease. Neuroimage 2020; 208: 116459.

[15] Suriya, M., Chandran, V., & Sumithra, M. G. Enhanced deep convolutional neural network for malarial parasite classification. Int J Comput Appl 2019; 1-10.

[16] Hemanth, D. J., Vijila, C. K. S., Selvakumar, A. I., & Anitha, J. Performance improved iteration-free artificial neural networks for abnormal magnetic resonance brain image classification. Neurocomputing 2014; 130: 98-107.

[17] Liu M, Li F, Yan H, et al. A multi-model deep convolutional neural network for automatic hippocampus segmentation and classification in Alzheimer's disease. NeuroImage 2020; 208: 116459.

[18] Ben Ahmed, O., Benois-Pineau, J., Allard, M., Ben Amar, C., & Catheline, G. Classification of Alzheimer's disease subjects from MRI using hippocampal visual features. Multimed Tools Appl 2015; 74(4): 1249-1266.

[19] Klöppel, S., Stonnington, C. M., Chu, C., Draganski, B., Scahill, R. I., Rohrer, J. D., ... & Frackowiak, R. S. Automatic classification of MR scans in Alzheimer's disease. Brain 2008; 131(3): 681-689.

[20] Farooq A, Anwar S, Awais M, Rehman S. A deep CNN based multi-class classification of Alzheimer's disease using MRI. Paper presented at the 2017 IEEE International Conference on Imaging Systems and Techniques (IST); 2017.

[21] Jongkreangkrai, C., Vichianin, Y., Tocharoenchai, C., Arimura, H., & Alzheimer's Disease Neuroimaging Initiative. Computer-aided classification of Alzheimer's disease based on support vector machine with combination of cerebral image features in MRI. In Journal of physics: conference series, March, 2016; 694(1): 012036.
[22] Moradi, E., Pepe, A., Gaser, C., Huttunen, H., Tohka, J., & Alzheimer's Disease Neuroimaging Initiative. Machine learning framework for early MRI-based Alzheimer's conversion prediction in MCI subjects. Neuroimage 2015; 104: 398-412.
[23] Feng W, Halm-Lutterodt NV, Tang H, et al. Automated MRIbased deep learning model for detection of Alzheimer's disease process. Int J Neural Syst 2020; 30(06): 2050032.
[24] Lerch, J. P., Pruessner, J., Zijdenbos, A. P., Collins, D. L., Teipel, S. J., Hampel, H., & Evans, A. C. Automated cortical thickness measurements from MRI can accurately separate Alzheimer's patients from normal elderly controls. Neurobiol Aging 2008; 29(1): 23-30.
[25] Cheng, B., Liu, M., Shen, D., Li, Z., & Zhang, D. Multi-domain transfer learning for early diagnosis of Alzheimer's disease. Neuroinformatics 2017; 15(2): 115-132.
[26] Sarraf S, Tofighi G. Deep learning-based pipeline to recognize Alzheimer's disease using fMRI data. Paper presented at the 2016 Future Technologies Conference (FTC); 2016.
[27] Billones, C. D., Demetria, O. J. L. D., Hostallero, D. E. D., & Naval, P. C. DemNet: a convolutional neural network for the detection of Alzheimer's disease and mild cognitive impairment. In 2016 IEEE region 10 conference (TENCON), November, 2016; pp. 3724-3727. IEEE.
[28] Khagi B, Kwon GR. 3D CNN design for the classification of Alzheimer's disease using brain MRI and PET. IEEE Access 2020; 8:217830-217847.
[29] Payan, A., & Montana, G. Predicting Alzheimer's disease: a neuroimaging study with 3D convolutional neural networks 2015; arXiv preprint arXiv:1502.02506.
[30] Hosseini-Asl, E., Gimel'farb, G., & El-Baz, A. Alzheimer's disease diagnostics by a deeply supervised adaptable 3D convolutional network 2016; arXiv preprint arXiv:1607.00556.
[31] Lama RK, Gwak J, Park J-S, Lee S-W. Diagnosis of Alzheimer's disease based on structural MRI images using a regularized extreme learning machine and PCA features. J Healthc Eng 2017; 5485080.
[32] Hon, M., & Khan, N. M. Towards Alzheimer's disease classification through transfer learning. In 2017 IEEE International conference on bioinformatics and biomedicine (BIBM), November, 2017; pp. 1166-1169. IEEE.
[33] Oh K, Chung Y-C, Kim KW, Kim W-S, Oh I-S. Classification and visualization of Alzheimer's disease using volumetric convolutional neural network and transfer learning. Sci Rep 2019; 9(1): 1-16.
[34] Eroglu, Y., Yildirim, M., & Cinar, A. mRMR-based hybrid convolutional neural network model for classification of Alzheimer's disease on brain magnetic resonance images. Int J Imaging Syst Technol 2022; 32(2): 517-527.
[35] Sarvesh D. Alzheimer's Dataset: Available from: https://www.kaggle.com/datasets/tourist55/alzheimers-dataset-4-class-of-images, 2019.
[36] Selvaraju, R. R., Cogswell, M., Das, A., Vedantam, R., Parikh, D., & Batra, D. Grad-cam: Visual explanations from deep networks via gradient-based localization. In Proceedings of the IEEE international conference on computer vision, 2017; pp. 618-626.
[37] Selvaraju, R. R., Das, A., Vedantam, R., Cogswell, M., Parikh, D., & Batra, D. Grad-CAM: Why did you say that?, 2016; arXiv preprint arXiv:1611.07450.
[38] Y. Bengio, A. Courville, and P. Vincent. Representation learning: A review and new perspectives. IEEE transactions on pattern analysis and machine intelligence 2013; 35(8):1798–1828.
[39] Mahendran, A., & Vedaldi, A. Visualizing deep convolutional neural networks using natural pre-images. Int J Comput Vis. 2016; 120(3): 233-255.
[40] Yu, X., Zeng, N., Liu, S., & Zhang, Y. D. Utilization of DenseNet201 for diagnosis of breast abnormality. Mach Vis Appl 2019; 30(7): 1135-1144.
[41] Tan, M., & Le, Q. Efficientnet: Rethinking model scaling for convolutional neural networks. In International conference on machine learning, May, 2019; pp. 6105-6114.
[42] Zahangir Alom, M., Taha, T. M., Yakopcic, C., Westberg, S., Sidike, P., Shamima Nasrin, M., ... & Asari, V. K. The history began from AlexNet: a comprehensive survey on deep learning approaches, 2018; arXiv e-prints, arXiv-1803.
[43] Jin, M., & Deng, W. Predication of different stages of Alzheimer's disease using neighborhood component analysis and ensemble decision tree. J Neurosci Methods 2018; 302, 35-41.
[44] Banerjee, C., Mukherjee, T., & Pasiliao Jr, E. An empirical study on generalizations of the ReLU activation function. In Proceedings of the 2019 ACM Southeast Conference, April, 2019; pp. 164-167.
[45] Özbay, E., Çinar, A., & Özbay, F. A. 3D Human Activity Classification with 3D Zernike Moment Based Convolutional, LSTM-Deep Neural Networks. Trait du Signal 2021; 38(2): 269-280.
[46] Yang, W., Wang, K., & Zuo, W. Neighborhood component feature selection for high-dimensional data. J Comput 2012; 7(1): 161-168.
[47] Carr, D. B., Goate, A., Phil, D., & Morris, J. C. Current concepts in the pathogenesis of Alzheimer's disease. The American journal of medicine 1997; 103(3): 3S-10S.
[48] Abuhmed, T., El-Sappagh, S., & Alonso, J. M. Robust hybrid deep learning models for Alzheimer's progression detection. Knowl.-Based Syst. 2021; 213: 106688.

[49] El-Sappagh, S., Saleh, H., Sahal, R., Abuhmed, T., Islam, S. R., Ali, F., & Amer, E. Alzheimer's disease progression detection model based on an early fusion of cost-effective multimodal data. Future Gener Comput Syst 2021; 115: 680-699.
[50] McKhann, G. M., Knopman, D. S., Chertkow, H., Hyman, B. T., Jack Jr, C. R., Kawas, C. H., ... & Phelps, C. H. The diagnosis of dementia due to Alzheimer's disease: Recommendations from the National Institute on Aging-Alzheimer's Association workgroups on diagnostic guidelines for Alzheimer's disease. Alzheimer's & dementia 2011; 7(3): 263-269.
[51] Hirni, D. I., Kivisaari, S. L., Monsch, A. U., & Taylor, K. I. Distinct neuroanatomical bases of episodic and semantic memory performance in Alzheimer's disease. Neuropsychologia 2013; 51(5): 930-937.
[52] Petrella, J. R., Wang, L., Krishnan, S., Slavin, M. J., Prince, S. E., Tran, T. T. T., & Doraiswamy, P. M. Cortical deactivation in mild cognitive impairment: high-field-strength functional MR imaging. Radiology 2007; 245(1): 224-235.
[53] Zhu, X., Schuff, N., Kornak, J., Soher, B., Yaffe, K., Kramer, J. H., ... & Weiner, M. W. Effects of Alzheimer disease on fronto-parietal brain N-acetyl aspartate and myo-inositol using magnetic resonance spectroscopic imaging. Alzheimer Dis Assoc Disord 2006; 20(2): 77.
[54] Özbay, E. An active deep learning method for diabetic retinopathy detection in segmented fundus images using artificial bee colony algorithm. Artif Intell Rev 2023; 56: 3291–3318.
[55] Özbay, E. Transformatör-Tabanlı Evrişimli Sinir Ağı Modeli Kullanarak Twitter Verisinde Saldırganlık Tespiti. Konya Mühendislik Bilimleri Dergisi 2022; 10(4): 986-1001.
[56] Özbay, F. A., & Özbay, E. A new approach for gender detection from voice data: Feature selection with optimization methods. J Fac Eng Archit Gazi Univ 2023; 38(2): 1179-1192.
[57] Odusami, M., Maskeliūnas, R., & Damaševičius, R. An Intelligent System for Early Recognition of Alzheimer's Disease Using Neuroimaging Sensors 2022; 22(3): 740.
[58] Razzak, I., Naz, S., Ashraf, A., Khalifa, F., Bouadjenek, M. R., & Mumtaz, S. Mutliresolutional ensemble PartialNet for Alzheimer detection using magnetic resonance imaging data. Int J Intell Syst 2022; 37(10): 6613-6630.